



Published in final edited form as:

Pain. 2020 July ; 161(7): 1636–1649. doi:10.1097/j.pain.0000000000001846.

Distribution of functional opioid receptors in human dorsal root ganglion neurons

Jamie K Moy¹, Jane E Hartung¹, Melissa G Duque¹, Rob Friedman¹, Vidhya Nagarajan¹, Emanuel Loeza-Alcocer¹, H. Richard Koerber¹, Thomas Christoph², Wolfgang Schröder², Michael S Gold^{1,*}

¹Department of Neurobiology, University of Pittsburgh School of Medicine, Pittsburgh, PA, United States

²Department of Translational Science & Pain Disease Understanding, Grünenthal GmbH, Aachen, Germany

Abstract

Preclinical evidence has highlighted the importance of the μ -opioid peptide (MOP) receptor on primary afferents for both the analgesic actions of MOP receptor agonists, as well as the development of tolerance, if not opioid-induced hyperalgesia. There is also growing interest in targeting other opioid peptide receptor subtypes (δ -opioid peptide (DOP), κ -opioid peptide (KOP), and nociceptin/orphanin-FQ opioid peptide (NOP)) on primary afferents, as alternatives to MOP receptors, that may not be associated with as many deleterious side effects. Nevertheless, results from several recent studies of human sensory neurons indicate that while there are many similarities between rodent and human sensory neurons, there may also be important differences. Thus, the purpose of the present study was to assess the distribution of opioid receptor subtypes among human sensory neurons. A combination of pharmacology, patch-clamp electrophysiology, Ca^{2+} imaging, and single-cell semi-quantitative polymerase chain reaction (qPCR) were employed. Our results suggest that functional MOP-like receptors are present in approximately 50% of human dorsal root ganglion (DRG) neurons. DOP-like receptors were detected in a subpopulation largely overlapping that with MOP-like receptors. Furthermore, KOP-like and NOP-like receptors are detected in a large proportion (44% and 40%, respectively) human DRG neurons with KOP receptors also overlapping with MOP receptors at a high rate (83%). Our data confirm that all four opioid receptor subtypes are present and functional in human sensory neurons, where the overlap of DOP, KOP, and NOP receptors with MOP receptors suggests that activation of these other opioid receptor subtypes may also have analgesic efficacy.

*Corresponding author Michael S Gold, University of Pittsburgh, 203 Lothrop St, BST W1451, Pittsburgh, PA 15213, 412-383-5367, msg22@pitt.edu.

Author contributions: JKM contributed to the experimental design, collected and analyzed data wrote the first draft of the manuscript. JEH, MGD, and RF collected and analyzed data. VN and ELA contributed to the collection and analysis of data. HRK, TC, and WS contributed to the experimental design and analysis of data. MSG contributed to the experimental design, data collection and analysis, and the preparation of the manuscript.

Competing interests: M. S. Gold has been a consultant to Grünenthal GmbH, Germany. T. Christoph and W. Schröder are employees of Grünenthal GmbH, Germany.

Data and materials availability: Yes

Keywords

mu-; delta-; kappa-; nociceptin/orphanin-FQ; co-expression

Introduction

While much of what we know about the properties of nociceptive afferents was obtained from the study of rodent sensory neurons, a number of recent studies of human sensory neurons have shown that in addition to important similarities between rodent and human sensory neurons [11; 28; 30], there are marked differences as well [7; 34; 41; 52; 72; 73] ranging from gene expression [12; 41; 52] to pharmacology and biophysical properties [12; 71; 72]. The issue of species differences may be a particularly important question to address in the context of opioid receptors both because of the ongoing opioid crisis in the United States and because of several recent high-profile papers highlighting the importance of opioid receptors on primary afferent neurons to the analgesic action of these drugs as well as the development of tolerance. Evidence has accumulated that opioid receptor subtypes other than the μ -opioid peptide (MOP[9]) receptor (the primary target for morphine and related compounds), such as the δ -opioid peptide (DOP, [1; 49]) receptor, κ -opioid peptide (KOP, [33; 60]) receptor, and nociceptin/orphanin-FQ opioid peptide (NOP, [10; 19; 23]) receptor may serve as analgesic targets devoid of the deleterious consequences associated with MOP receptor agonists. Indeed, large differences have been documented between rodents and primates in opioid expression profiles [6; 10; 24]. Thus, the purpose of the present study was to characterize the distribution of functional opioid receptor subtypes in human dorsal root ganglion (DRG) neurons.

The possibility DOP, KOP, and or NOP receptors may serve as alternative therapeutic targets for the treatment of pain is largely supported by rodent data demonstrating the analgesic efficacy of peripherally administered DOP [35], KOP [8; 33; 60], and NOP [13; 23; 25] receptor agonists. Whether this reflects agonist activity on a subpopulation of afferents overlapping that expressing MOP receptor, remains an area of controversy for DOP receptors with conflicting evidence of both a high level of receptor co-expression in small diameter peptidergic DRG neurons [21; 40; 53; 56; 61; 70] and a pattern of expression that is largely non-overlapping [47; 48]. Data from both rat and mouse are more consistent and suggest that while there is clearly overlap in the expression of MOP and KOP receptors, KOP receptors are more widely distributed [21; 29] [54]. In contrast, *in situ* analysis showed that NOP receptors are predominantly expressed in a non-overlapping subpopulation of medium to large cell body diameter DRG neurons [37].

Our results support the suggestion that DOP, KOP and NOP receptor agonists may be viable alternatives to MOP receptor agonists for the treatment of pain.

Materials and Methods

Human DRG collection and culture

Lumbar 4 and 5 DRG from human donors were obtained with the consent of their next of kin to use their family member's tissue for research purposes. Collection and study of the DRG was approved by the University of Pittsburgh Committee for Oversight of Research and Clinical Training Involving Decedents. Consent was obtained by Center for Organ Recovery and Education (CORE) staff, as was the collection of tissue. DRG were collected as previously described in [73] and immediately placed in ice cold collection media (in mM: 124.5 NaCl, 5 KCl, 1.2 MgSO₄, 1 CaCl₂, and 30 HEPES) pH with NaOH to 7.2. DRG were then cleaned of connective tissue, cut into small (~1 mm³) pieces, and enzymatically treated with 6.25% (w/v) collagenase P (Sigma-Aldrich, St Louis, MO) for 1 – 2.5 h at 37°C prior to mechanical dissociation. These final steps were initiated for all donors within 6 hours post cross-clamp (the time at which systemic circulation was stopped). Dissociation and plating protocols [73] as well as solution components [73] were followed as previously described. Neurons were studied between 12 h – 5 days after plating.

Patch-clamp electrophysiology

Standard whole cell patch clamp techniques were used to record voltage-gated Ca²⁺ currents in human DRG neurons. Data were collected with HEKA EPC10 controlled by Patchmaster (v 2×90.5) software (HEKA Elektronik GmbH, Lambrecht/Pfalz Germany). Data were acquired at 5–20 kHz and filtered at 1–4 kHz. Borosilicate glass (WPI, Sarasota, FL) electrodes were 1–2 MΩ when filled with the electrode solution containing (in mM): 130 Choline-Cl, 3 KCl, 5 BaCl₂, 0.6 MgCl₂, 10 HEPES, 10 glucose. The pH was adjusted to 7.4 with 10% w/v tris-base, and the osmolarity was adjusted to 320 mosmol kg⁻¹ with sucrose. The electrode solution consisted of (in mM): 110 TEA-MES, 40 TEA-Cl, 2 MgCl₂, 1 CaCl₂, 11 EGTA, 10 HEPES, 2 Mg-ATP, and 1 Li-GTP. The pH was adjusted to 7.2 with 10% w/v tris-base, and the osmolarity was adjusted to 310 mosmol kg⁻¹ with sucrose.

Ca²⁺ Imaging

Human DRG neurons were loaded with 2.5 μM Ca²⁺ indicator fura-2 AM ester with 0.025% w/v Pluronic F-127 in normal bath solution (NB) for 30 min at 37°C. NB consisted of (in mM): 130 NaCl, 3 KCl, 2.5 CaCl₂, 0.6 MgCl₂, 10 HEPES, 10 glucose. The pH was adjusted to 7.4 with 10% w/v tris-base, and the osmolarity was adjusted to 320 mosmol kg⁻¹ with sucrose. Neurons were then placed in a recording chamber continuously perfused with NB. Fluorescence data were acquired on a PC running Metafluor software (Molecular Devices, Sunnyvale, CA) via an EMCCD camera (Photometrics, Tucson, AZ; model QuantEM 512SC). For Fura-2 imaging, the ratio (*R*) of fluorescence emission (510 nm) in response to 340/380nm excitation (controlled by a DG-4 (Sutter Instrument, Novato, CA)) was acquired at 1 Hz during application of KCl (50 mM) or capsaicin (500 nM), which were applied through a computer-controlled, piezo-driven perfusion system (Warner Instruments, Hamden, CT, USA, Fast-Step Model SF-77B). The advantage of this system is that with the cells in the field of view under the direct flow from the perfusion pipette perfused with a flow rate of approximately 1mL/min, it is possible to completely exchange the solution around the cells very rapidly without having to exchange the entire recording chamber

volume. The rate of exchange was confirmed with cell free patch electrodes in which the holding current was measured following application and wash of a solution containing 50 mM KCl. The holding current change was complete within 20 ms and stable with each change of solution (data not shown). Neurons were considered responsive to KCl and/or capsaicin if their application was associated with an increase in fluorescence > two standard deviations above baseline. Similarly, neurons were considered responsive to opioid receptor agonists if the KCl-evoked response was changed > two standard deviations from the baseline KCl-evoked response. Data are plotted as a change in fluorescence (ΔF) over baseline fluorescence (F).

Drugs

DAMGO ([D-Ala², N-MePhe⁴, Gly-ol]-enkephalin), DADLE ([D-Ala², D-Leu⁵]-enkephalin), dynorphin, nociceptin/orphanin-FQ, CTOP (D-Phe-Cys-Tyr-D-Trp-Orn-Thr-Pen-Thr-NH₂), and naltrindole were dissolved in water. Nor-binaltorphimine (nor-BNI), bpV(Phen), and SB 612111 were dissolved in DMSO. Naloxone and (\pm)-J113397 were dissolved in ethanol. All test agents were dissolved as 100x to 1000x stocks and stored at -20°C until use. Opioid receptor agonists and antagonists were obtained from Sigma-Aldrich (St Louis, MO) and/or Tocris Bioscience (Bristol, UK), while bpV(Phen) was obtained from Cayman Chemicals (Ann Arbor, MI).

Single-cell semi-quantitative reverse transcriptase polymerase chain reaction (RT-qPCR)

Dissociated human DRG neurons were collected with large bore (~40 μ m) pipettes, expelled into tubes containing 3 μ l of extraction buffer, and stored at -80°C until processed. Transcripts from single cells were reverse transcribed and linearly preamplified using the MessageBOOSTER kit for cell lysate (Epicentre). After preamplification, the products were cleaned with RNA Cleaner & Concentrator-5 columns (Zymo Research) and transcript levels were quantified using qPCR with optimized primers and SsoAdvanced SYBR Green Master Mix (BioRad). Cycle-time (Ct) values were determined using regression. Quantification threshold was determined to be inter-replicate average of 32 Ct, the point where replicates have a 95% chance of reoccurring, and the GAPDH threshold for cell inclusion was set to 23 Ct to ensure we could detect transcripts a thousand-times less prevalent than GAPDH. Bacterial RNA for Lys was added to each mixture as an external control. Primer sequences are listed in Table 2.

Statistical Analyses

In accordance to previous studies involving human DRG, no *a priori* analyses were performed to estimate the number of donors necessary to complete this study. The statistical tests used to compare groups and/or treatments are indicated in the figure legends. Unless otherwise specified data are presented as mean \pm SEM.

Results

Over 1500 DRG neurons from 54 donors were studied for the characterization of opioid receptors. These donors consisted of 23 females and 31 males ranging between 18 to 77 years old with a median age of approximately 45 years. The majority of the donors were

white with the exception of 3 African Americans, 1 Asian American, and 1 Native Hawaiian. A breakdown of the donors by sex, age, and race can be found in Table 1.

The contribution of voltage-gated Ca²⁺ channels to the actions of opioids and KCl-evoked Ca²⁺ transients in human DRG neurons

Rodent data suggests that the primary mechanism underlying the analgesic action of spinal opioids is the inhibition of transmitter release from primary afferents [26; 38] secondary to the inhibition of voltage-gated Ca²⁺ currents (VGCC, [22; 63]). The analgesic effects of inhibiting transmitter release from central terminals is in contrast to the inhibition of VGCC in peripheral terminals, which while suppressing the efferent release of transmitter in the periphery, does not appear to influence nociceptor excitability and consequently nociceptive threshold [51]. And while the efferent release of transmitter may contribute to the inflammatory response and consequently pain associated with tissue injury [64], this distinction helps explain why peripheral administration of opioid receptor agonists have been generally shown to have little analgesic effect in the absence of tissue injury [2; 27; 59]. Thus, while other functional assays could be used to screen for the anti-hyperalgesic actions of opioid receptor agonists [15], the focus on VGCC inhibition in the present study should be considered a screen for potential analgesic effects, particularly if agonists were administered spinally. To confirm that a similar mechanism occurs in human DRG neurons, we assessed the impact of the selective MOP receptor agonist, [D-Ala², N-MePhe⁴, Gly-ol]-enkephalin (DAMGO, 1 μM), on VGCC evoked in human DRG neurons with patch-clamp electrophysiology. DAMGO significantly reduced VGCC (FIG 1A) by an average of $37.9 \pm 5.9\%$ ($n = 10$). There was a small-decay in the magnitude of inhibition with a three-minute application of DAMGO, but while recovery from inhibition was relatively slow, it was largely complete after three minutes of washing (FIG 1A, bottom). To at least begin to assess whether other opioid receptor agonists act via a comparable mechanism, we screened for the effects of the KOP agonist (dynorphin) and NOP agonist nociceptin on VGCC in human DRG neurons. Currents were inhibited by dynorphin in two of three neurons tested and nociceptin in two of four neurons tested (data not shown). Two mechanisms have been described underlying G-protein-coupled receptor-induced suppression of VGCC: a protein kinase C-dependent process that is relatively slow to develop and reverse, that is associated with a decrease in the number of functional channels in the membrane [57; 67; 68; 74], and a membrane delimited rapid Gβγ-dependent mechanism, involving the displacement of the voltage-gated Ca²⁺ channel β subunit [18; 65], and a depolarizing shift in the voltage dependence of channel activation. Because it is possible to reverse this second form of inhibition with a depolarizing voltage step, a process referred to as pre-pulse potentiation, we screened for the latter mechanism of VGCC inhibition with a pre-pulse protocol (FIG 1B, top). Consistent with a Gβγ-dependent mechanism of VGCC inhibition, a pre-pulse to +70 mV partially reversed DAMGO-induced inhibition of VGCCs (FIG 1B, bottom).

Because of the capability to screen multiple neurons at the same time for their responses to opioid receptor agonists with Ca²⁺ imaging, we next sought to confirm that KCl-evoked Ca²⁺ transients, as assessed with fura-2 microfluorimetry, was dependent on Ca²⁺ influx through VGCCs. After establishing a stable baseline response to KCl in normal bath solution (NB) (FIG 1C), the bath solution was changed to a nominally Ca²⁺-free bath

solution (0 Ca^{2+} but no Ca^{2+} chelator added). In the presence of Ca^{2+} -free bath the evoked Ca^{2+} transient was reduced by $95.7 \pm 1.2\%$ (FIG 1D, $n = 29$). Moreover, when high and low threshold VGCC blockers, $100 \mu\text{M CdCl}_2$ and $100 \mu\text{M NiSO}_4$, respectively, were added to NB, the evoked Ca^{2+} transient was reduced (FIG 1E) by $74.6 \pm 1.7\%$ (FIG 1F, $n = 9$). Together these data suggest that KCl-evoked Ca^{2+} transients can be used to screen for the presence of functional opioid receptors in human DRG neurons.

Distribution of functional μ -opioid (MOP) receptors among human DRG neurons

The distribution of MOP receptors among rodent sensory neurons has been well described functionally, where in mouse and rat DRG neurons, it appears to be primarily restricted to a subpopulation of small diameter neurons also responsive to the algogen capsaicin [44; 50; 58; 62]. To assess the distribution of functional MOP receptors among human DRG neurons, we assessed the impact of DAMGO on KCl-evoked Ca^{2+} transients (FIG 2A). Based on our criterion for considering a neuron responsive to an agonist (i.e., a change in evoked transient $>$ two standard deviations from the baseline KCl response), 30 of 58 neurons tested (51.7%) were responsive to DAMGO. In these neurons, the average maximal suppression of the evoked transient was $42 \pm 5\%$ (FIG 2B). Additionally, 15 of these neurons were tested for capsaicin sensitivity and 12 were responsive, suggesting that the majority of the neurons are nociceptive.

The inhibitory actions of DAMGO were concentration dependent (FIG 2B). The lowest concentration of DAMGO with which we were able to detect an effect was 30 nM. However, both the magnitude of the inhibition, and the proportion of neurons responsive to DAMGO (FIG 2B, inset) increased in response to concentrations of DAMGO higher than 30 nM. The EC_{50} for DAMGO was 56 nM. Consistent with the suggestion that DAMGO is a selective MOP receptor agonist, the MOP receptor antagonist, naloxone ($1 \mu\text{M}$) (FIG 2C, top) significantly attenuated the DAMGO-induced suppression of the evoked Ca^{2+} transients to $13.3 \pm 1.2\%$ (FIG 2D, bottom), but did not affect the proportion of DAMGO responders (FIG 2D, top). Curiously, the MOP receptor antagonist CTOP ($10 \mu\text{M}$) (FIG 2C, bottom) alone produced an inhibition of $31.1 \pm 4.0\%$ ($n = 11$; data not shown) of the evoked Ca^{2+} transient. This effect was seen across 5 donors as well as different drug batches from different vendors. Further characterization revealed that the CTOP-induced inhibition of the evoked Ca^{2+} transient is not blocked by naloxone ($n = 10$, $p=0.89$, paired t-test; data not shown). CTOP attenuated the evoked Ca^{2+} transient with an EC_{50} of $0.55 \mu\text{M}$ with a maximal inhibition of 31% at $3 \mu\text{M}$ (data not shown). This inhibition was unlikely to be a solution exchange artifact either, as there was no change in background fluorescence associated with the addition of CTOP containing solution. Nevertheless, CTOP ($10 \mu\text{M}$) decreased the proportion of DAMGO-responsive neurons (FIG 2D, top), as well as the magnitude of the DAMGO-induced suppression of the evoked Ca^{2+} transient (to $20.1 \pm 2.8\%$). Furthermore, when neurons were challenged with DAMGO again following wash of CTOP, there was a significant increase in the magnitude of the DAMGO-induced suppression of the evoked Ca^{2+} transient (FIG 2D, bottom). In contrast to CTOP, naloxone alone, had no detectable influence on either resting Ca^{2+} or KCl-evoked Ca^{2+} transients, in the vast majority of neurons tested. However, in neurons isolated from one donor a naloxone-induced increase in intracellular Ca^{2+} was detected (not shown). Curiously, this

particular donor had a past medical history of opioid abuse, and died of apparent overdose. These data are in line with evidence suggesting that the MOP receptor signaling is altered after exposure to MOP receptor agonists [17; 32; 69]. We observed no age-dependent influence on the number of DAMGO responders (>65yo; n = 4 donors vs <30yo; n = 3 donors). However, there was a significant influence of sex on the number of neurons responsive to DAMGO (females n = 8 donors; 44/97 (45.4%) vs males n = 7 donors; 99/153 (64.7%), **p=0.003, chi-squared).

Distribution of functional δ -opioid (DOP) receptors among human DRG neurons

We next sought to assess the distribution of DOP receptor among human DRG neurons. DOP receptor signaling among DRG neurons remains one of the more controversial topics in the opioid literature. One line of evidence from both rat and mouse suggests that DOP receptors are present in a subpopulation of DRG neurons largely overlapping with that expressing MOP receptors [21; 40; 61]. In these neurons, however, DOP receptors are not normally present on the plasma membrane, and is only trafficked to the membrane following high levels of activity [43] and/or changes in the balance of phosphatase/kinase activity [53]. In contrast, an opposing line of evidence from the mouse suggests DOP receptors are present in a population of medium to large neurons distinct from that expressing MOP receptors, where it is present in the plasma membrane even at rest [47; 48]. To begin to assess the presence of DOP receptors in human DRG neurons, we started with the putative DOP receptor selective agonist, SNC80, in an experiment similar to that used with DAMGO, with the exception that following wash of SNC80, we could also determine whether the neuron was responsive to DAMGO (FIG 3A). Similar to the bulk of rodent data, we found that under basal conditions very few (1 of 42 (2.4%)) neurons from one donor responded to SNC80 at 1 μ M. At 3 and 10 μ M, we observed a marked increase in the number of responsive neurons and fractional inhibition of the evoked Ca^{2+} transient (FIG 3B and inset). Such a high proportion of SNC80 responders was consistent with previous data suggesting that SNC80 has off-target effects at concentrations not much higher than that needed to produce a maximal DOP receptor response [48]. However, assuming 1 μ M SNC80 is still selective for DOP receptors, we next assessed the impact of pre-incubating DRG neurons in bpV(Phen) (10 μ M for 30 minutes at 37°C), a phosphatase and tensin homolog (PTEN) inhibitor. This was based on recent data suggesting that under basal conditions, the balance of PI3Kinase to PTEN activity is such that DOP receptors are retained in the Golgi, while an increase in receptor phosphorylation is sufficient to enable DOP receptor trafficking to the plasma membrane [53]. Consistent with the rodent data, we found that PTEN inhibition significantly increased the proportion of neurons responsive to SNC80 (1 μ M) (12/25 (48%)) compared to vehicle treated neurons (2/15 (13.3%)) (FIG 3C, top). This increase in the proportion of SNC80 responders did not appear to be associated with an increase in the magnitude of the response (FIG 3C, bottom). Neurons tested with SNC80 were also tested with DAMGO (1 μ M) and capsaicin (500 nM). The distributions of vehicle and bpV(Phen) treated neurons responsive to each test agent are plotted (FIG 3D). Of note, the majority of SNC80 responsive neurons were also responsive to DAMGO and capsaicin (FIG 3D). To test our assumption about the selectivity of 1 μ M SNC80 for DOP receptors, we assessed the impact of a selective DOP receptor antagonist, naltrindole [39] (3 and 10 μ M) on the response to SNC80 (FIG 3E). Interestingly, like CTOP, naltrindole alone at 10 μ M also

produced a small but significant ($16.2 \pm 1.6\%$) reduction in the evoked transient. Regardless of this effect, naltrindole at 3 and 10 μM had no detectable impact on the proportion of bpV(Phen)-treated neurons responsive to SNC80 (FIG 3F, top). However, naltrindole at 10 μM decreased the magnitude of SNC80-induced inhibition of the evoked transient (FIG 3F, bottom). These results suggest that naltrindole is not as potent against human DOP receptors in their native environment, as it is in the rodent or heterologous expression systems. Age differences were not determined due to the lack of age range of donors screened with SNC80 (no donors under 30yo were screened). There was, however, the suggestion of a sex difference detected in the number of neurons responsive to SNC80 (females $n = 2$ donors; 9/25 (36%) vs males $n = 3$ donors; 6/56 (10.7%), $**p=0.007$, chi-squared).

To further explore the distribution of DOP receptors among human DRG neurons, we assessed the impact of a second DOP receptor agonist, DADLE (FIG 4A). In contrast to SNC80, we saw no effect of bpV(Phen) on the proportion of neurons that were responsive to DADLE (1 μM , bpV(Phen)- 18/40 (45%) vs vehicle- 9/26 (34.6%) FIG 4B, top). Pre-treatment with bpV(Phen) had no detectable influence on the magnitude of the DADLE-induced decrease in the evoked Ca^{2+} transient (FIG 4B, bottom). As with SNC80, neurons tested with DADLE were also tested with DAMGO (1 μM) and capsaicin (500 nM). The distributions of vehicle and bpV(Phen) treated neurons responsive to each test agent are plotted (FIG 4C). Of note, the majority of DADLE responsive neurons were also responsive to DAMGO, and at least half were responsive to capsaicin. Additionally, we repeated the naltrindole experiment with DADLE (FIG 4D). This time, we used naltrindole at concentrations ranging from 1 – 10 μM . Regardless of antagonist concentration, there was no significant influence of naltrindole on the proportion of DADLE-responders (FIG 4E, top). However, the magnitude of the DADLE-induced suppression of the evoked Ca^{2+} transient was significantly attenuated by both 3 (data not shown) and 10 μM naltrindole (FIG 4E, bottom). Age and sex differences were not determined due to the lack of age range (only 1 donor was younger than 30yo) and sex across donors screened with DADLE (only 1 male was screened).

Distribution of functional κ -opioid (KOP) receptors among human DRG neurons

Dynorphin was used as a KOP receptor agonist to assess the distribution of functional KOP receptors among human DRG neurons as was described for MOP and DOP receptors (FIG 5A). The effects of dynorphin were concentration dependent with both the proportion of dynorphin responders, and the magnitude of the response, increasing between 30 nM and 1 μM (FIG 5B and inset). The EC_{50} for dynorphin-induced suppression of the evoked Ca^{2+} transient was 297 nM. Interestingly, while the majority of neurons responsive to dynorphin (1 μM) were also responsive to DAMGO, less than half were responsive to capsaicin (FIG 5C). Finally, to confirm the involvement of KOP receptors in the actions of dynorphin, we employed the KOP receptor selective antagonist nor-BNI (FIG 4D). While nor-BNI had no detectable influence on the resting or evoked Ca^{2+} transient, there was a significant reduction in both the proportion of dynorphin responders (FIG 5E, top), and the magnitude of the dynorphin-induced suppression of the evoked Ca^{2+} transient (FIG 5E, bottom). Age and sex differences were not determined due to the lack of age range (all donors were

between the age of 35 – 64yo) and sex across donors screened with dynorphin (only 1 male was screened).

Distribution of functional nociceptin/orphanin-FQ-opioid (NOP) receptors among human DRG neurons

Lastly, we assessed the distribution of functional NOP receptors among human DRG neurons as with the other opioid receptor subtypes (FIG 6A). Nociceptin was used as the NOP receptor selective agonist, due to its low affinity for other opioid receptor subtypes [42]. As with the other opioid receptor agonists, the effects of nociceptin were concentration dependent, with both the proportion of NOP receptor agonist responders and the magnitude of the effect increasing with nociceptin concentrations between 30 nM and 1 μ M (FIG 6B and inset). The EC_{50} for the nociceptin-induced suppression of the evoked Ca^{2+} transient was 75 nM. A subpopulation of neurons was also tested for sensitivity to nociceptin, DAMGO, and capsaicin. While it was not clear whether it was a reflection of donor variability or some other factor, the proportion of neurons responsive to nociceptin when also tested for sensitivity to DAMGO and capsaicin, was higher (~65%, $p = 0.04$, chi-square test) than the proportion of neurons responsive to nociceptin, when the response to this ligand was tested alone (~40%), regardless of whether the neuron was first challenged with nociceptin or DAMGO. Regardless, more than half of the nociceptin-responsive neurons were also responsive to DAMGO, while a small majority were responsive to capsaicin (FIG 6C).

Similar to the analyses of putatively selective MOP, DOP, and KOP receptor agonists, we assessed the impact of NOP receptor antagonists on the actions of nociceptin. We started with J113397 (10 μ M, FIG 6D and E), and found that J113397 alone inhibited the evoked Ca^{2+} transient (FIG 6E) in 18/38 neurons with an average inhibition of $22.7 \pm 2.8\%$ (data not shown). Nevertheless, in the presence of the antagonist only a small proportion of the neurons tested (5/36) were responsive to nociceptin (1 μ M, FIG 6D). Furthermore, following wash of the antagonist, the magnitude of the nociceptin-induced suppression of the evoked Ca^{2+} transient was larger than in the presence of this antagonist (FIG 6F). Because of the effect of J113397 alone on the evoked Ca^{2+} transient, we tried a second NOP antagonist, SB 612111 (3 μ M, FIG 6G). Unlike J113397, SB 612111 alone did not inhibit evoked Ca^{2+} transients and had no influence on the proportion of nociceptin responsive neurons (FIG 6D). However, the magnitude of the nociceptin-induced suppression of the evoked Ca^{2+} transient was significantly attenuated by SB 612111 (22.0% vs 28.4%, $p = 0.0094$, $n = 16$). Furthermore, when neurons were challenged with nociceptin again following wash of SB 612111, there was a significant increase in the magnitude of the nociceptin-induced suppression of the evoked Ca^{2+} transient (FIG 6H). There was the suggestion of an influence of age on the number of nociceptin responders ($>65yo$ $n = 2$ donors; 37/52 (71.1%) neurons vs $<30yo$ $n = 2$ donors; 14/40 (35%) neurons, *** $p=0.0005$, chi-squared). Sex differences were not determined due to the lack of sex across multiple donors screened with nociceptin (only 1 female was screened).

Expression of opioid receptor subtypes among human DRG neurons

As a complimentary approach to the analysis of the distribution of functional opioid receptor subtypes among human DRG neurons, we performed a single cell PCR analysis of opioid receptor subtypes among neurons from 5 donors (FIG 7A). Donors consisted of 3 males and 2 females age ranging from 22 yo to 70 yo (FIG 7B), four donors were white/Caucasian and the fifth was African-American. We found on average OPRM1 was expressed in $24.0 \pm 3.7\%$; OPRD1 in $4.5 \pm 1.3\%$; OPRK1 in $49.7 \pm 7.5\%$ and OPRL1 in $48.4 \pm 6.1\%$, and TRPV1 in $96.5 \pm 1.6\%$ of neurons.

Discussion

The purpose of this study was to determine the distribution of functional opioid receptor subtypes among human DRG neurons. We found that activation of human DRG MOP receptors results in the inhibition of VGCCs. Consistent with this mode of action, opioid receptor agonists suppressed the Ca^{2+} transient evoked by a brief application of 50 mM K^{+} . Agonist-induced suppression of evoked Ca^{2+} transients were concentration dependent at least for MOP, KOP, and NOP receptor agonists, and the effects of each receptor subtype selective agonist were attenuated by receptor subtype specific antagonists. The pharmacology of DOP receptors was more complex. Two DOP receptor agonists were used that appeared to have different pharmacological properties: pretreatment with bpV(Phen) increased the number of responders to SNC80 but the number of responders to DADLE was as high in untreated neurons as that responsive to SNC80 following bpV(Phen) treatment. However, the impact of both DOP receptor agonists was antagonized by the DOP receptor selective antagonist naltrindole. Overlap of functional MOP receptor with the other opioid receptors subtypes was relatively high for DOP receptors as well as for KOP and NOP receptors. The proportion of neurons expressing KOP and NOP receptors as detected with single-cell qPCR was generally consistent with functional data. In contrast, MOP receptor mRNA was detected in ~half the number of neurons in which a response to DAMGO was detected, and the disconnect was even larger for DOP receptors. Consistent with previous studies of human DRG neurons, this analysis of functional opioid receptors revealed similarities and potentially important species differences with respect to the distribution and pharmacology of these important receptors.

There were clearly similarities between our results and previous data from the study of rodent sensory neurons. Our results are largely consistent with evidence indicating that the analgesic effect of opioids is due to the inhibition of VGCC on primary afferents. The pharmacology of MOP, KOP, and NOP receptors in human DRG neurons are roughly comparable to that previously reported in rodent. The distribution of MOP and KOP receptor subtypes among human DRG neurons also appears to be comparable to that in rodent [47; 54]. Lastly, the distribution of NOP receptors among human DRG neurons is comparable to that previously described in rat (and human) where the receptor is present in both TRPV1+ and TRPV1- neurons [3].

The most notable difference between human DRG neurons and previous data from rodents was the significant attenuation of the evoked Ca^{2+} transient by MOP, DOP and NOP receptor selective antagonists CTOP, naltrindole, and J113397 [66]. Furthermore, despite

evidence suggesting that the antagonists used are both potent and relatively selective, they were not nearly as effective as predicted. This was true regardless of whether the antagonist inhibited the evoked Ca^{2+} transient underscoring the potential importance of native environment on receptor pharmacology. A potentially related observation was that the combination of Cd^{2+} and Ni^{2+} did not block as much of the evoked Ca^{2+} transient as would have been predicted from rodent data [36]. This suggests that either high K^{+} activates a VGCC-independent Ca^{2+} influx pathway, or like the opioid receptors studied here, and our previous data with voltage-gated Na^{+} currents [72], nicotinic acetyl choline receptors [71] and GABA_A receptors [73] in human DRG neurons, the pharmacology of VGCCs in human DRG neurons is different from that observed in rodent neurons or heterologous expression systems.

Similarly, while the naltrindole data are consistent with the suggestion that both SNC80 (1 μM) and DADLE (1 μM) effects were DOP receptor mediated, the observation that PTEN inhibition increased the number of SNC80 but not DADLE responders, suggests that bpV(Phen) modified the signaling pathway activated by SNC80 [16] rather than releasing DOP receptors from Golgi [53]. Consistent with this suggestion, there is evidence of ligand directed signaling differences between rodent and human opioid receptors (albeit for KOP receptors [45; 46]), as well as evidence that receptor phosphorylation influences whether agonists activate G-protein receptor or β -arrestin pathways. Thus, it is possible that bpV(Phen) enables SNC80 to activate a G-protein-dependent pathway that is normally engaged by DADLE activation of DOP receptors in human DRG neurons. Such a mechanism could help explain the limited clinical success of DOP receptor selective agonists [55], particularly, if the compounds tested have a pharmacological profile similar to that observed for SNC80. Nevertheless, regardless of why PTEN inhibition is needed for SNC80 but not DADLE activity, the presence of functional DOP receptors in ~50% of human DRG neurons largely overlapping that with MOP receptors is consistent with older rat [21] and mouse [62] data, as well as more recent mouse data [31; 53; 61]. Such a distribution is opposed to that described in other mouse studies suggesting that MOP and DOP receptors are in non-overlapping subpopulations of DRG neurons [47; 48], and mediate modality specific analgesia. The low level of DOP receptor mRNA was detected in human DRG neurons is also consistent with the former lines of evidence, where receptor activation appears to be necessary to drive an increase in DOP receptor mRNA [43], but not the latter (where DOP receptors appear to be constitutively expressed at high levels). One potential explanation for the differences in these data sets is that the majority of data supporting the non-overlapping constitutive pattern of DOP receptor expression were based on a mouse line in which the OPRD1 had been modified to generate a GFP tagged DOP receptor [4; 47; 48]; this mutation may not only impact receptor trafficking, but could also influence the pattern of expression.

There were at least two results from our single cell PCR analysis that are worth noting. The first is the apparent disconnect between the pattern of expression for MOP, DOP, and TRPV1, and the distribution of functional receptors. This was most notable for DOP receptors at one extreme and TRPV1 at the other, but was also true for MOP receptors. That is, as noted we obtained evidence of functional DOP receptors in ~50% of DRG neurons, while the mRNA was detected in 5%. In contrast, capsaicin evoked Ca^{2+} transients were

only observed in 54% (421/775) of neurons tested, while TRPV1 mRNA was detected in 96% of neurons. As suggested above, the pattern of OPRD1 expression is similar to that reported in rats [21] and consistent with activity-dependent regulation of expression [43]. The relatively low level of OPRD1 expression observed at the single cell level is also consistent with the relatively low level of expression previously reported with RNAseq analysis of whole DRG [12]. In contrast, the pattern of TRPV1 expression is consistent, at least in part with an injury-induced upregulation of TRPV1 associated with putting the neurons in culture, given evidence from rat suggesting nerve injury results in an increase in TRPV1 expression in subpopulations of neurons that do not normally express this receptor [5; 14; 20]. This highlights a caveat of this study, which is that it was not only performed on tissue obtained after death, but after frank injury to the neurons studied. Nevertheless, the patterns of opioid receptor gene expression at the whole ganglia level is at least consistent with our single cell data and argues against injury-induced changes in the patterns observed [41]. Minimally, however, these data highlight the caution that should be employed when interpreting gene expression data, particularly with the level of sensitivity now possible with RNAseq based approaches.

The second interesting observation was associated with the donor to donor variability. While the majority of the donors passed away from stroke or cardiac arrest, a few donors had a history of opioid abuse including a donor with low OPRM1 expression (FIG 7B). In addition to the variability between donors, there are other potential explanations for the differences between previously described opioid receptor distribution in rodents and the current study in human DRG. First, the majority of rodent studies were collected in males of similar age with limited genetic variability, whereas our study consists of approximately 43% females (Table 1). Second, recovery of tissue from experimental animals is relatively time-locked, while there was considerably more variability in the timing around the recovery and processing of tissue from organ donors. Third, rodents have relatively limited life experiences, while this is certainly not the case for donors (Table 1).

Our current study is the first to assess the distribution of functional opioid receptor subtypes in human DRG neurons. Our data highlight both similarities and potentially important differences between humans and rodents both with respect to the distribution of opioid receptor subtypes, and the impact of the reagents routinely used to study these receptors. The similarities noted validate the continued use of rodents for the study of opioid receptor pharmacology, at least receptors not genetically modified. However, the differences, in particular those related to receptor pharmacology, suggest that an analysis of the effects of opioid compounds currently approved for clinical use may shed some light on differences in clinical utility. The differences also suggest that it will be important, if not essential, to screen novel pharmacological compounds against human receptors in their native environment, prior to initiating clinical trials.

Supplementary Material

Refer to Web version on PubMed Central for supplementary material.

Acknowledgements:

This work was supported by Grünenthal GmbH. It was also supported by grants from the National Institutes of Health F32NS110148 (JKM) F32NS103231 (JEH) T32NS073548 (JEH and JKM), R01NS096705 (HRK), R01NS083347 and R01DK107966 (MSG). We acknowledge the Center for Organ Recovery and Education (CORE) for their help in coordinating receipt of tissue from organ donors. We thank the donor family members for graciously consenting to the use of their loved one's tissue for research purposes.

REFERENCES

- [1]. Abdelhamid EE, Sultana M, Portoghese PS, Takemori AE. Selective blockage of delta opioid receptors prevents the development of morphine tolerance and dependence in mice. *J Pharmacol Exp Ther* 1991;258(1):299–303. [PubMed: 1649297]
- [2]. Aley KO, Levine JD. Different mechanisms mediate development and expression of tolerance and dependence for peripheral mu-opioid antinociception in rat. *J Neurosci* 1997;17(20):8018–8023. [PubMed: 9315920]
- [3]. Anand P, Yiangou Y, Anand U, Mukerji G, Sinisi M, Fox M, McQuillan A, Quick T, Korchev YE, Hein P. Nociceptin/orphanin FQ receptor expression in clinical pain disorders and functional effects in cultured neurons. *Pain* 2016;157(9):1960–1969. [PubMed: 27127846]
- [4]. Bardoni R, Tawfik VL, Wang D, Francois A, Solorzano C, Shuster SA, Choudhury P, Betelli C, Cassidy C, Smith K, de Nooij JC, Mennicken F, O'Donnell D, Kieffer BL, Woodbury CJ, Basbaum AI, MacDermott AB, Scherrer G. Delta Opioid Receptors Presynaptically Regulate Cutaneous Mechanosensory Neuron Input to the Spinal Cord Dorsal Horn. *Neuron* 2014;81(6):1443.
- [5]. Biggs JE, Yates JM, Loeschner AR, Clayton NM, Boissonade FM, Robinson PP. Changes in vanilloid receptor 1 (TRPV1) expression following lingual nerve injury. *Eur J Pain* 2007;11(2):192–201. [PubMed: 16542859]
- [6]. Bowen CA, Fischer BD, Mello NK, Negus SS. Antagonism of the antinociceptive and discriminative stimulus effects of heroin and morphine by 3-methoxynaltrexone and naltrexone in rhesus monkeys. *J Pharmacol Exp Ther* 2002;302(1):264–273. [PubMed: 12065726]
- [7]. Chang W, Berta T, Kim YH, Lee S, Lee SY, Ji RR. Expression and Role of Voltage-Gated Sodium Channels in Human Dorsal Root Ganglion Neurons with Special Focus on Nav1.7, Species Differences, and Regulation by Paclitaxel. *Neurosci Bull* 2018;34(1):4–12. [PubMed: 28424991]
- [8]. Cowan A, Kehner GB, Inan S. Targeting Itch with Ligands Selective for kappa Opioid Receptors. *Handb Exp Pharmacol* 2015;226:291–314. [PubMed: 25861786]
- [9]. Cox BM, Christie MJ, Devi L, Toll L, Traynor JR. Challenges for opioid receptor nomenclature: IUPHAR Review 9. *British journal of pharmacology* 2015;172(2):317–323. [PubMed: 24528283]
- [10]. Cremeans CM, Gruley E, Kyle DJ, Ko MC. Roles of mu-opioid receptors and nociceptin/orphanin FQ peptide receptors in buprenorphine-induced physiological responses in primates. *J Pharmacol Exp Ther* 2012;343(1):72–81. [PubMed: 22743574]
- [11]. Davidson S, Copits BA, Zhang J, Page G, Ghetti A, Gereau RW. Human sensory neurons: Membrane properties and sensitization by inflammatory mediators. *Pain* 2014;155(9):1861–1870. [PubMed: 24973718]
- [12]. Davidson S, Golden JP, Copits BA, Ray PR, Vogt SK, Valtcheva MV, Schmidt RE, Ghetti A, Price TJ, Gereau RWt. Group II mGluRs suppress hyperexcitability in mouse and human nociceptors. *Pain* 2016;157(9):2081–2088. [PubMed: 27218869]
- [13]. Ding H, Hayashida K, Suto T, Sukhtankar DD, Kimura M, Mendenhall V, Ko MC. Spinal actions of nociceptin/orphanin FQ, morphine and substance P in regulating pain and itch in non-human primates. *Br J Pharmacol* 2015;172(13):3302–3312. [PubMed: 25752320]
- [14]. Fukuoka T, Tokunaga A, Tachibana T, Dai Y, Yamanaka H, Noguchi K. VR1, but not P2X(3), increases in the spared L4 DRG in rats with L5 spinal nerve ligation. *Pain* 2002;99(1–2):111–120. [PubMed: 12237189]

- [15]. Gold MS, Levine JD. DAMGO inhibits prostaglandin E2-induced potentiation of a TTX-resistant Na⁺ current in rat sensory neurons in vitro. *Neurosci Lett* 1996;212(2):83–86. [PubMed: 8832644]
- [16]. Grecco HE, Schmick M, Bastiaens PI. Signaling from the living plasma membrane. *Cell* 2011;144(6):897–909. [PubMed: 21414482]
- [17]. Groer CE, Schmid CL, Jaeger AM, Bohn LM. Agonist-directed interactions with specific beta-arrestins determine mu-opioid receptor trafficking, ubiquitination, and dephosphorylation. *J Biol Chem* 2011;286(36):31731–31741. [PubMed: 21757712]
- [18]. Herlitz S, Garcia DE, Mackie K, Hille B, Scheuer T, Catterall WA. Modulation of Ca²⁺ channels by G-protein beta gamma subunits. *Nature* 1996;380(6571):258–262. [PubMed: 8637576]
- [19]. Hu E, Calo G, Guerrini R, Ko MC. Long-lasting antinociceptive spinal effects in primates of the novel nociceptin/orphanin FQ receptor agonist UFP-112. *Pain* 2010;148(1):107–113. [PubMed: 19945794]
- [20]. Hudson LJ, Bevan S, Wotherspoon G, Gentry C, Fox A, Winter J. VR1 protein expression increases in undamaged DRG neurons after partial nerve injury. *Eur J Neurosci* 2001;13(11):2105–2114. [PubMed: 11422451]
- [21]. Ji RR, Zhang Q, Law PY, Low HH, Elde R, Hokfelt T. Expression of mu-, delta-, and kappa-opioid receptor-like immunoreactivities in rat dorsal root ganglia after carrageenan-induced inflammation. *J Neurosci* 1995;15(12):8156–8166. [PubMed: 8613750]
- [22]. Jiang YQ, Andrade A, Lipscombe D. Spinal morphine but not ziconotide or gabapentin analgesia is affected by alternative splicing of voltage-gated calcium channel CaV2.2 pre-mRNA. *Mol Pain* 2013;9:67. [PubMed: 24369063]
- [23]. Kiguchi N, Ding H, Ko MC. Central N/OFQ-NOP Receptor System in Pain Modulation. *Adv Pharmacol* 2016;75:217–243. [PubMed: 26920014]
- [24]. Ko MC, Divin MF, Lee H, Woods JH, Traynor JR. Differential in vivo potencies of naltrexone and 6beta-naltrexol in the monkey. *J Pharmacol Exp Ther* 2006;316(2):772–779. [PubMed: 16258020]
- [25]. Ko MC, Woods JH, Fantegrossi WE, Galuska CM, Wichmann J, Prinszen EP. Behavioral effects of a synthetic agonist selective for nociceptin/orphanin FQ peptide receptors in monkeys. *Neuropsychopharmacology* 2009;34(9):2088–2096. [PubMed: 19279568]
- [26]. Lembeck F, Donnerer J. Opioid control of the function of primary afferent substance P fibres. *Eur J Pharmacol* 1985;114(3):241–246. [PubMed: 2415368]
- [27]. Levine JD, Taiwo YO. Involvement of the mu-opiate receptor in peripheral analgesia. *Neuroscience* 1989;32(3):571–575. [PubMed: 2557556]
- [28]. Li Y, Adamek P, Zhang H, Tatsui CE, Rhines LD, Mrozkova P, Li Q, Kosturakis AK, Cassidy RM, Harrison DS, Cata JP, Sapire K, Zhang H, Kennamer-Chapman RM, Jawad AB, Ghetti A, Yan J, Palecek J, Dougherty PM. The Cancer Chemotherapeutic Paclitaxel Increases Human and Rodent Sensory Neuron Responses to TRPV1 by Activation of TLR4. *J Neurosci* 2015;35(39):13487–13500. [PubMed: 26424893]
- [29]. Maekawa K, Minami M, Yabuuchi K, Toya T, Katao Y, Hosoi Y, Onogi T, Satoh M. In situ hybridization study of mu- and kappa-opioid receptor mRNAs in the rat spinal cord and dorsal root ganglia. *Neurosci Lett* 1994;168(1–2):97–100. [PubMed: 8028801]
- [30]. Megat S, Ray PR, Moy JK, Lou TF, Barragan-Iglesias P, Li Y, Pradhan G, Wangzhou A, Ahmad A, Burton MD, North RY, Dougherty PM, Khoutorsky A, Sonenberg N, Webster KR, Dussor G, Campbell ZT, Price TJ. Nociceptor Translational Profiling Reveals the Regulator-Rag GTPase Complex as a Critical Generator of Neuropathic Pain. *J Neurosci* 2019;39(3):393–411. [PubMed: 30459229]
- [31]. Metcalf MD, Yekkirala AS, Powers MD, Kitto KF, Fairbanks CA, Wilcox GL, Portoghese PS. The delta opioid receptor agonist SNC80 selectively activates heteromeric mu-delta opioid receptors. *ACS Chem Neurosci* 2012;3(7):505–509. [PubMed: 22860219]
- [32]. Miess E, Gondin AB, Yousuf A, Steinborn R, Mosslein N, Yang Y, Goldner M, Ruland JG, Bunemann M, Krasel C, Christie MJ, Halls ML, Schulz S, Canals M. Multisite phosphorylation

is required for sustained interaction with GRKs and arrestins during rapid mu-opioid receptor desensitization. *Sci Signal* 2018;11(539).

- [33]. Millan MJ. Kappa-opioid receptors and analgesia. *Trends Pharmacol Sci* 1990;11(2):70–76. [PubMed: 2156363]
- [34]. North RY, Li Y, Ray P, Rhines LD, Tatsui CE, Rao G, Johansson CA, Zhang H, Kim YH, Zhang B, Dussor G, Kim TH, Price TJ, Dougherty PM. Electrophysiological and transcriptomic correlates of neuropathic pain in human dorsal root ganglion neurons. *Brain* 2019;142(5):1215–1226. [PubMed: 30887021]
- [35]. Pasquinucci L, Parenti C, Turnaturi R, Arico G, Marrazzo A, Prezzavento O, Ronsisvalle S, Georgoussi Z, Fourla DD, Scoto GM, Ronsisvalle G. The benzomorphan-based LP1 ligand is a suitable MOR/DOR agonist for chronic pain treatment. *Life Sci* 2012;90(1–2):66–70. [PubMed: 22100511]
- [36]. Perez-Reyes E. Molecular physiology of low-voltage-activated t-type calcium channels. *Physiol Rev* 2003;83(1):117–161. [PubMed: 12506128]
- [37]. Pettersson LM, Sundler F, Danielsen N. Expression of orphanin FQ/nociceptin and its receptor in rat peripheral ganglia and spinal cord. *Brain Res* 2002;945(2):266–275. [PubMed: 12126889]
- [38]. Pohl M, Lombard MC, Bourgoin S, Carayon A, Benoliel JJ, Mauborgne A, Besson JM, Hamon M, Cesselin F. Opioid control of the in vitro release of calcitonin gene-related peptide from primary afferent fibres projecting in the rat cervical cord. *Neuropeptides* 1989;14(3):151–159. [PubMed: 2559354]
- [39]. Portoghese PS, Sultana M, Takemori AE. Naltrindole, a highly selective and potent non-peptide delta opioid receptor antagonist. *Eur J Pharmacol* 1988;146(1):185–186. [PubMed: 2832195]
- [40]. Rau KK, Caudle RM, Cooper BY, Johnson RD. Diverse immunocytochemical expression of opioid receptors in electrophysiologically defined cells of rat dorsal root ganglia. *J Chem Neuroanat* 2005;29(4):255–264. [PubMed: 15927787]
- [41]. Ray P, Torck A, Quigley L, Wangzhou A, Neiman M, Rao C, Lam T, Kim JY, Kim TH, Zhang MQ, Dussor G, Price TJ. Comparative transcriptome profiling of the human and mouse dorsal root ganglia: an RNA-seq-based resource for pain and sensory neuroscience research. *Pain* 2018;159(7):1325–1345. [PubMed: 29561359]
- [42]. Reinscheid RK, Nothacker HP, Bourson A, Ardati A, Henningsen RA, Bunzow JR, Grandy DK, Langen H, Monsma FJ Jr., Civelli O. Orphanin FQ: a neuropeptide that activates an opioidlike G protein-coupled receptor. *Science* 1995;270(5237):792–794. [PubMed: 7481766]
- [43]. Rowan MP, Ruparel NB, Patwardhan AM, Berg KA, Clarke WP, Hargreaves KM. Peripheral delta opioid receptors require priming for functional competence in vivo. *Eur J Pharmacol* 2009;602(2–3):283–287. [PubMed: 19063879]
- [44]. Saloman JL, Scheff NN, Snyder LM, Ross SE, Davis BM, Gold MS. Gi-DREADD Expression in Peripheral Nerves Produces Ligand-Dependent Analgesia, as well as Ligand-Independent Functional Changes in Sensory Neurons. *J Neurosci* 2016;36(42):10769–10781. [PubMed: 27798132]
- [45]. Schattauer SS, Kuhar JR, Song A, Chavkin C. Nalfurafine is a G-protein biased agonist having significantly greater bias at the human than rodent form of the kappa opioid receptor. *Cell Signal* 2017;32:59–65. [PubMed: 28088389]
- [46]. Schattauer SS, Miyatake M, Shankar H, Zietz C, Levin JR, Liu-Chen LY, Gurevich VV, Rieder MJ, Chavkin C. Ligand directed signaling differences between rodent and human kappa-opioid receptors. *J Biol Chem* 2012;287(50):41595–41607. [PubMed: 23086943]
- [47]. Scherrer G, Imamachi N, Cao YQ, Contet C, Mennicken F, O'Donnell D, Kieffer BL, Basbaum AI. Dissociation of the opioid receptor mechanisms that control mechanical and heat pain. *Cell* 2009;137(6):1148–1159. [PubMed: 19524516]
- [48]. Scherrer G, Tryoen-Toth P, Filliol D, Matifas A, Laustriat D, Cao YQ, Basbaum AI, Dierich A, Vonesh JL, Gaveriaux-Ruff C, Kieffer BL. Knockin mice expressing fluorescent delta-opioid receptors uncover G protein-coupled receptor dynamics in vivo. *Proc Natl Acad Sci U S A* 2006;103(25):9691–9696. [PubMed: 16766653]
- [49]. Schiller PW. Bi- or multifunctional opioid peptide drugs. *Life Sci* 2010;86(15–16):598–603. [PubMed: 19285088]

- [50]. Schroeder JE, McCleskey EW. Inhibition of Ca²⁺ currents by a mu-opioid in a defined subset of rat sensory neurons. *J Neurosci* 1993;13(2):867–873. [PubMed: 7678862]
- [51]. Shakhaneh J, Lynn B. Morphine inhibits antidromic vasodilatation without affecting the excitability of C-polymodal nociceptors in the skin of the rat. *Brain Res* 1993;607(1–2):314–318. [PubMed: 8481806]
- [52]. Sheahan TD, Valtcheva MV, McIlvried LA, Pullen MY, Baranger DAA, Gereau RWt. Metabotropic Glutamate Receptor 2/3 (mGluR2/3) Activation Suppresses TRPV1 Sensitization in Mouse, But Not Human, Sensory Neurons. *eNeuro* 2018;5(2).
- [53]. Shiwarski DJ, Tipton A, Giraldo MD, Schmidt BF, Gold MS, Pradhan AA, Puthenveedu MA. A PTEN-Regulated Checkpoint Controls Surface Delivery of delta Opioid Receptors. *J Neurosci* 2017;37(14):3741–3752. [PubMed: 28264976]
- [54]. Snyder LM, Chiang MC, Loeza-Alcocer E, Omori Y, Hachisuka J, Sheahan TD, Gale JR, Adelman PC, Sypek EI, Fulton SA, Friedman RL, Wright MC, Duque MG, Lee YS, Hu Z, Huang H, Cai X, Meerschaert KA, Nagarajan V, Hirai T, Scherrer G, Kaplan DH, Porreca F, Davis BM, Gold MS, Koerber HR, Ross SE. Kappa Opioid Receptor Distribution and Function in Primary Afferents. *Neuron* 2018;99(6):1274–1288 e1276. [PubMed: 30236284]
- [55]. Spahn V, Stein C. Targeting delta opioid receptors for pain treatment: drugs in phase I and II clinical development. *Expert Opin Investig Drugs* 2017;26(2):155–160.
- [56]. Spike RC, Puskar Z, Sakamoto H, Stewart W, Watt C, Todd AJ. MOR-1-immunoreactive neurons in the dorsal horn of the rat spinal cord: evidence for nonsynaptic innervation by substance P-containing primary afferents and for selective activation by noxious thermal stimuli. *Eur J Neurosci* 2002;15(8):1306–1316. [PubMed: 11994125]
- [57]. Stea A, Soong TW, Snutch TP. Determinants of PKC-dependent modulation of a family of neuronal calcium channels. *Neuron* 1995;15(4):929–940. [PubMed: 7576641]
- [58]. Taddese A, Nah SY, McCleskey EW. Selective opioid inhibition of small nociceptive neurons. *Science* 1995;270(5240):1366–1369. [PubMed: 7481826]
- [59]. Taiwo YO, Levine JD. Kappa- and delta-opioids block sympathetically dependent hyperalgesia. *J Neurosci* 1991;11(4):928–932. [PubMed: 2010815]
- [60]. Vanderah TW. Delta and kappa opioid receptors as suitable drug targets for pain. *Clin J Pain* 2010;26 Suppl 10:S10–15. [PubMed: 20026960]
- [61]. Wang HB, Zhao B, Zhong YQ, Li KC, Li ZY, Wang Q, Lu YJ, Zhang ZN, He SQ, Zheng HC, Wu SX, Hokfelt TG, Bao L, Zhang X. Coexpression of delta- and mu-opioid receptors in nociceptive sensory neurons. *Proc Natl Acad Sci U S A* 2010;107(29):13117–13122. [PubMed: 20615975]
- [62]. Werz MA, Grega DS, MacDonald RL. Actions of mu, delta and kappa opioid agonists and antagonists on mouse primary afferent neurons in culture. *J Pharmacol Exp Ther* 1987;243(1):258–263. [PubMed: 2822900]
- [63]. Werz MA, Macdonald RL. Opioid peptides decrease calcium-dependent action potential duration of mouse dorsal root ganglion neurons in cell culture. *Brain Res* 1982;239(1):315–321. [PubMed: 7093688]
- [64]. Willis WD Jr. Dorsal root potentials and dorsal root reflexes: a double-edged sword. *Exp Brain Res* 1999;124(4):395–421. [PubMed: 10090653]
- [65]. Womack MD, McCleskey EW. Interaction of opioids and membrane potential to modulate Ca²⁺ channels in rat dorsal root ganglion neurons. *J Neurophysiol* 1995;73(5):1793–1798. [PubMed: 7623080]
- [66]. Wu ZZ, Chen SR, Pan HL. Differential sensitivity of N- and P/Q-type Ca²⁺ channel currents to a mu opioid in isolectin B4-positive and -negative dorsal root ganglion neurons. *J Pharmacol Exp Ther* 2004;311(3):939–947. [PubMed: 15280436]
- [67]. Yang J, Tsien RW. Enhancement of N- and L-type calcium channel currents by protein kinase C in frog sympathetic neurons. *Neuron* 1993;10(2):127–136. [PubMed: 8382496]
- [68]. Zamponi GW, Bourinet E, Nelson D, Nargeot J, Snutch TP. Crosstalk between G proteins and protein kinase C mediated by the calcium channel alpha1 subunit. *Nature* 1997;385(6615):442–446. [PubMed: 9009192]

- [69]. Zhang L, Zhao H, Qiu Y, Loh HH, Law PY. Src phosphorylation of micro-receptor is responsible for the receptor switching from an inhibitory to a stimulatory signal. *J Biol Chem* 2009;284(4):1990–2000. [PubMed: 19029294]
- [70]. Zhang X, Bao L, Arvidsson U, Elde R, Hokfelt T. Localization and regulation of the delta-opioid receptor in dorsal root ganglia and spinal cord of the rat and monkey: evidence for association with the membrane of large dense-core vesicles. *Neuroscience* 1998;82(4):1225–1242. [PubMed: 9466442]
- [71]. Zhang X, Hartung JE, Friedman RL, Koerber HR, Belfer I, Gold MS. Nicotine Evoked Currents in Human Primary Sensory Neurons. *J Pain* 2019;20(7):810–818. [PubMed: 30659887]
- [72]. Zhang X, Priest BT, Belfer I, Gold MS. Voltage-gated Na(+) currents in human dorsal root ganglion neurons. *Elife* 2017;6.
- [73]. Zhang XL, Lee KY, Priest BT, Belfer I, Gold MS. Inflammatory mediator-induced modulation of GABAA currents in human sensory neurons. *Neuroscience* 2015;310:401–409. [PubMed: 26415765]
- [74]. Zhu Y, Ikeda SR. Modulation of Ca(2+)-channel currents by protein kinase C in adult rat sympathetic neurons. *J Neurophysiol* 1994;72(4):1549–1560. [PubMed: 7823085]

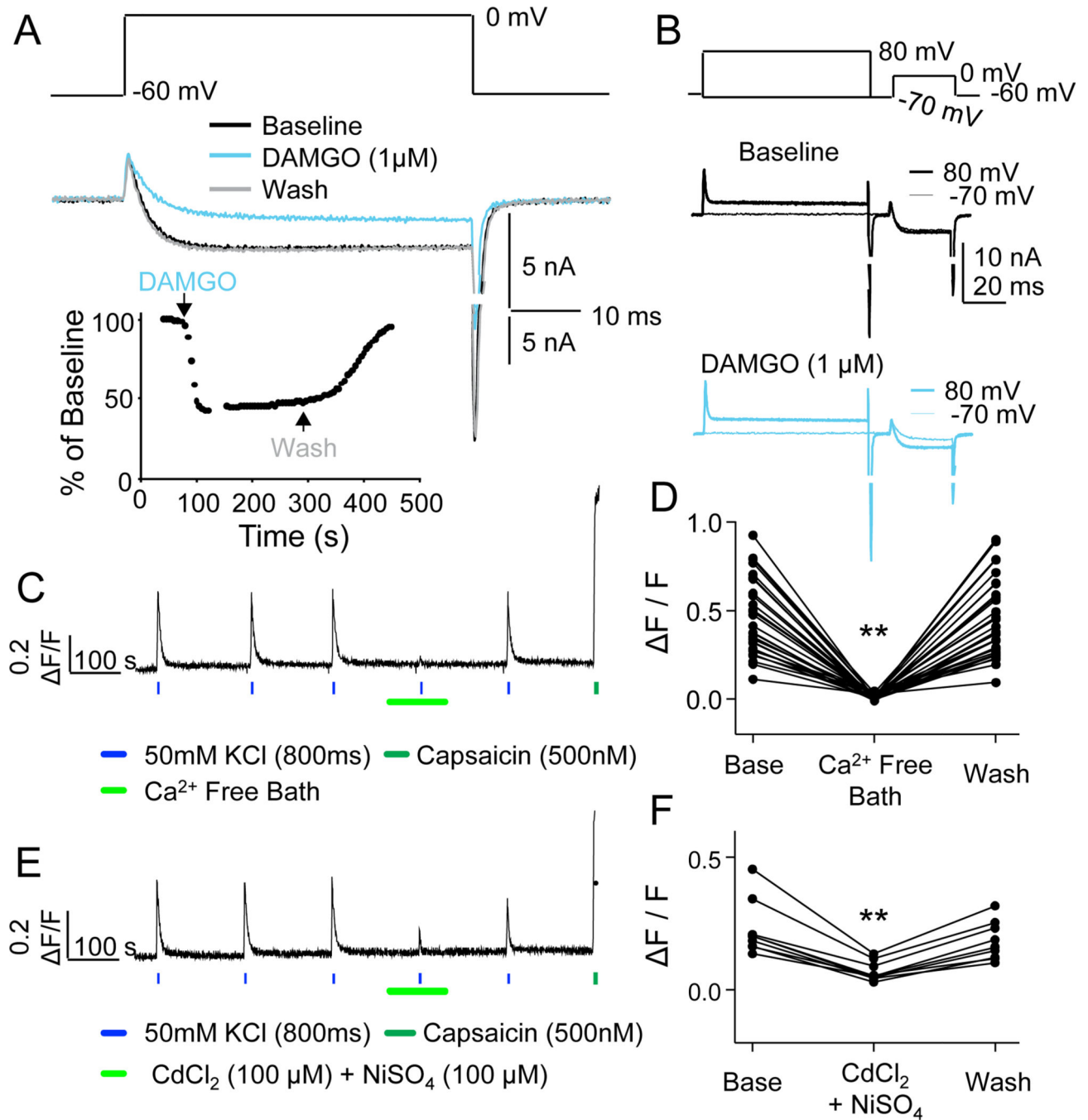


Figure 1. Voltage-gated Ca²⁺ currents (VGCCs) in human DRG neurons as a target for opioid receptor activation, and as a mechanism for initiating depolarization-induced increases in intracellular Ca²⁺.

A. VGCC were evoked from a holding potential of -60 mV, to a test potential of 0 mV, before and after the application of DAMGO ($1 \mu\text{M}$). Inset: A diary plot of the peak inward current before, during and after DAMGO as indicated. **B.** A pre-pulse potentiation protocol involving an 80 ms pre-pulse to either -70 mV (thin lines) or $+80$ mV (heavier lines) prior to a test pulse to 0 mV, was employed before (top traces) and after (bottom traces) the application of DAMGO. Current suppressed by DAMGO could be recovered by a pre-pulse

to +80 mV. **C.** Typical Ca^{2+} imaging protocol used to assess the impact of opioid receptor agonists on Ca^{2+} transients evoked with a depolarization associated with the application (800 ms) of 50 mM KCl. The evoked transient was reversibly eliminated by the application of a Ca^{2+} free bath solution. The neuron illustrated was responsive to capsaicin (500 nM). **D.** Pooled data from 23 neurons from three donors confirm the dependence of the depolarization evoked transient on Ca^{2+} influx ($F(1.3, 35.4) = 107.9$, $df=2$, $n=29$, $**p<0.01$, RM ANOVA). **E.** The depolarization evoked Ca^{2+} transient was also reversibly attenuated by the non-specific VGCC blockers Cd^{2+} (100 μM) and Ni^{2+} (100 μM). **F.** Pooled data from 9 neurons from 3 donors confirmed that the attenuation of the evoked Ca^{2+} transient was significant ($F(1.5, 11.7) = 37.3$, $df=2$, $n=9$, $**p=0.01$, RM ANOVA).

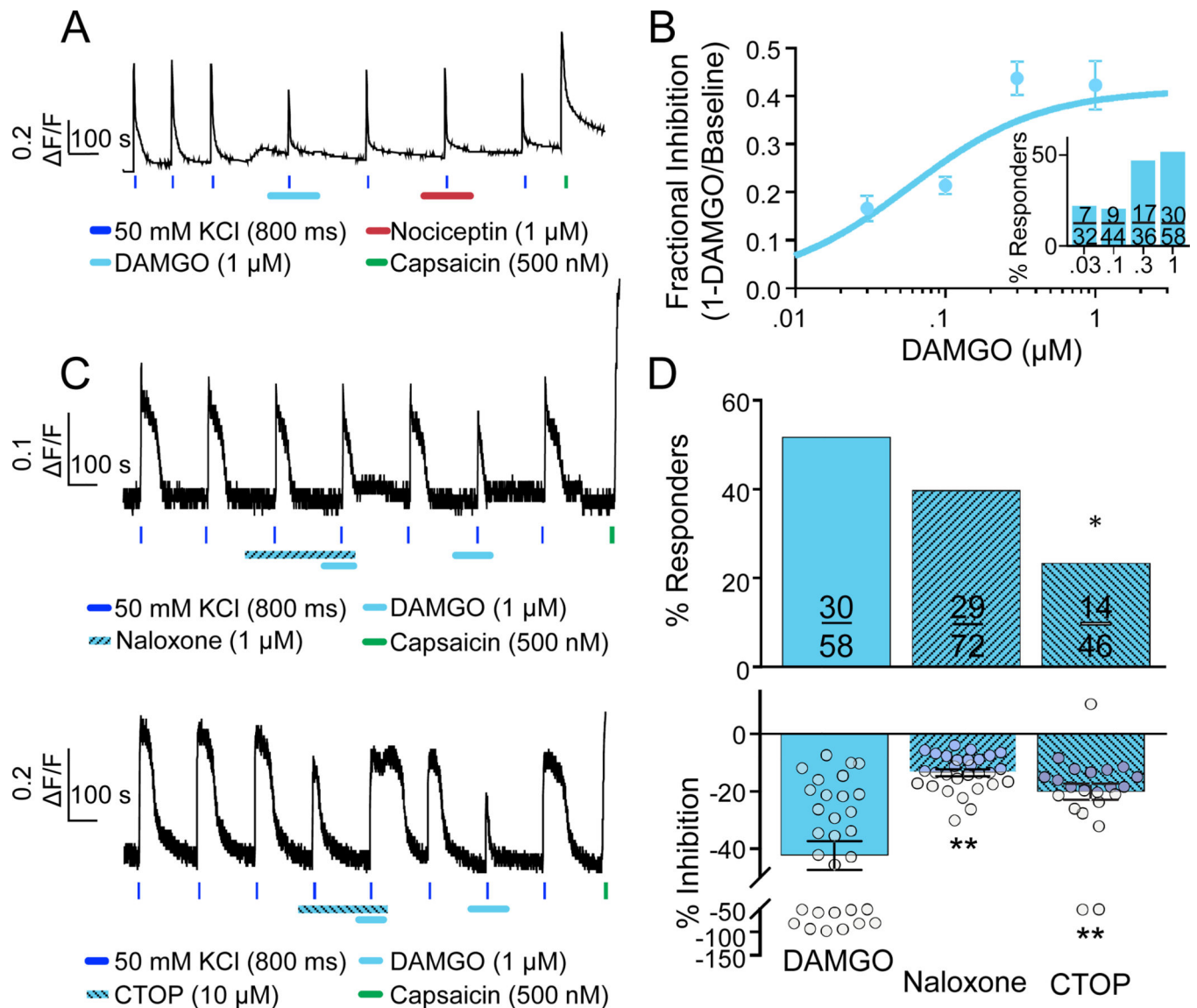


Figure 2. Characterization of functional MOP receptors in human DRG neurons.

A. DAMGO responsive neuron that was also responsive to capsaicin, but that appeared unresponsive to nociceptin. **B.** Pooled data from DAMGO responsive neurons challenged with DAMGO at concentrations between 30 nM and 1 μ M. Data were fitted with a Hill equation yielding an EC_{50} of 56 nM and a maximal inhibition of 40%. Inset: Percent of DAMGO responsive neurons (Responders) plotted as function of DAMGO concentration. **C.** The MOP receptor antagonists naloxone (top trace) and CTOP (bottom trace) attenuated the magnitude of DAMGO-mediated inhibition and/or percentage of DAMGO responsive neurons (Naloxone; $p=0.19$, chi-squared test. CTOP; $*p=0.045$, fisher's exact test). Interestingly, however, CTOP itself, significantly attenuated the evoked Ca^{2+} transient. **D.** Pooled data from neurons challenged with DAMGO alone, or DAMGO in the presence of either naloxone or CTOP ($P<0.01$, $F(2, 78)=17.03$, ANOVA, post-hoc Dunnett's test for multiple comparisons, $**p=0.01$).

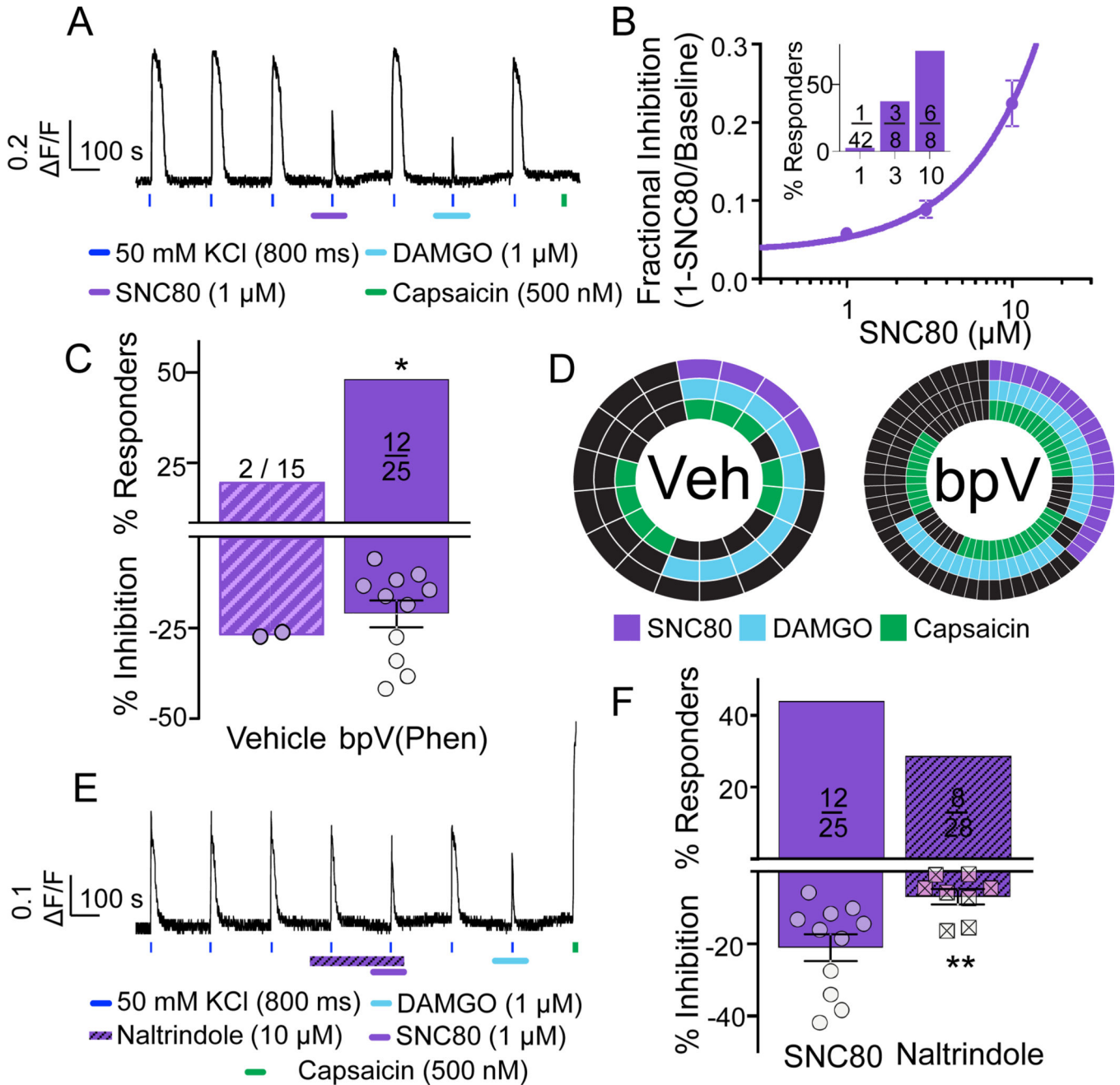


Figure 3. Characterization of DOP receptor agonist, SNC80, in human DRG neurons.
A. Example of a neuron pre-treated (for 30 min) with the PTEN inhibitor, bpV(Phen), that was responsive to SNC80 (1 μ M), DAMGO (1 μ M), and capsaicin (500 nM). **B.** Without pretreatment with bpV(Phen), very few neurons were responsive to SNC80 at a concentration of 1 μ M. However, the fractional inhibition and percentage of responsive neurons (inset) increased as the concentration of SNC80 was increased to 3 and 10 μ M. **C.** Pooled data of neurons pre-treated with bpV(Phen) or vehicle that were subsequently challenged with 1 μ M SNC80 ($p=0.026$, chi-square). **D.** Distribution of vehicle and bpV(Phen) treated neurons that were responsive to SNC80, DAMGO, and/or capsaicin. In

this and subsequent figures, each spoke in the wheel represents a single neuron. Of note, the vehicle wheel includes the 2/15 neurons responsive to SNC80 when challenged with the agonist alone, as well as the 2/2 neurons responsive to SNC80 when challenged with the agonist following application of naltrindole. **E.** Example of a neuron challenged with SNC80 following application of the DOP receptor antagonist naltrindole. The neuron was subsequently challenged with DAMGO and capsaicin. Note the inhibition associated with naltrindole alone. **F.** Pooled data of bpV(Phen) treated neurons that were subsequently challenged with SNC80 alone or following the application of naltrindole. While there was no significant influence of naltrindole on the percentage of neurons responsive to SNC80 ($p=0.24$, chi-square), the attenuation of the magnitude of the suppression of the evoked transient was significant ($t=2.97$, $df=17$, $**p=0.01$, unpaired t-test).

Author Manuscript

Author Manuscript

Author Manuscript

Author Manuscript

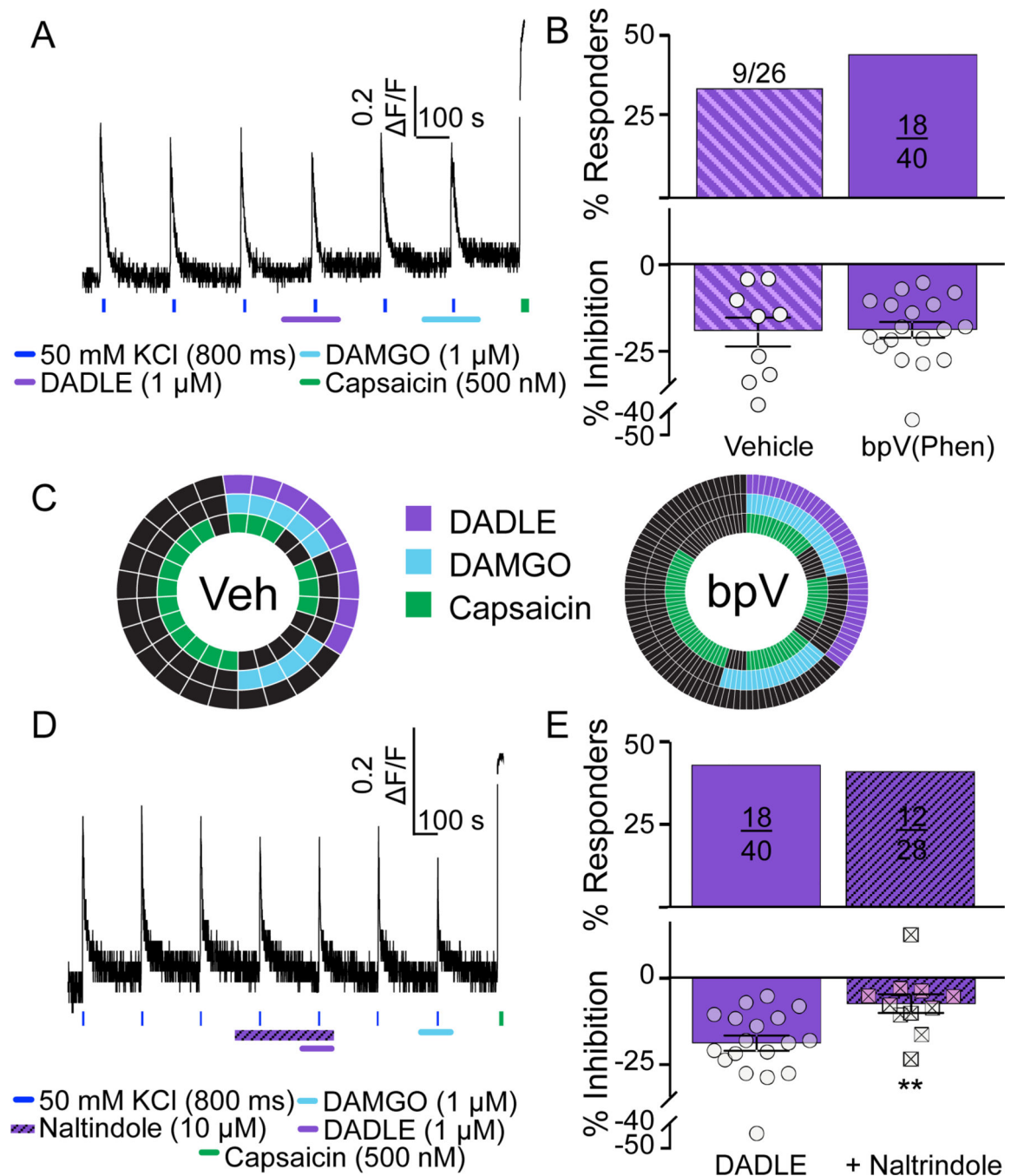


Figure 4. Further characterization functional DOP receptors with peptide agonist, DADLE, in human DRG neurons.

A. Example of Ca^{2+} signaling in neuron responsive to the DOP receptor agonist DADLE. This neuron was also responsive to DAMGO and capsaicin. **B.** In contrast to the influence of bpV(Phen) on the proportion of neurons responsive to SNC80, there was no detectable influence of PTEN inhibition on either the proportion of neurons responsive to DADLE ($p=0.40$, chi-squared), or the magnitude of the response ($t=0.16$, $df=25$, $p > 0.05$, t-test). **C.** Distribution of vehicle and bpV(Phen) treated neurons that were responsive to DADLE,

DAMGO, and/or capsaicin. **D.** Example of a neuron in which naltrindole attenuated the response to DADLE, that was also responsive to DAMGO and capsaicin. **E.** Pooled data from neurons challenged with DADLE alone or DADLE following the application of naltrindole. While there was no detectable influence of naltrindole on the proportion of neurons responsive to DADLE ($p=0.86$, chi-square), there was a significant attenuation of the magnitude of the DADLE effect (** $p=0.0037$, $t=3.183$, $df=27$, t-test).

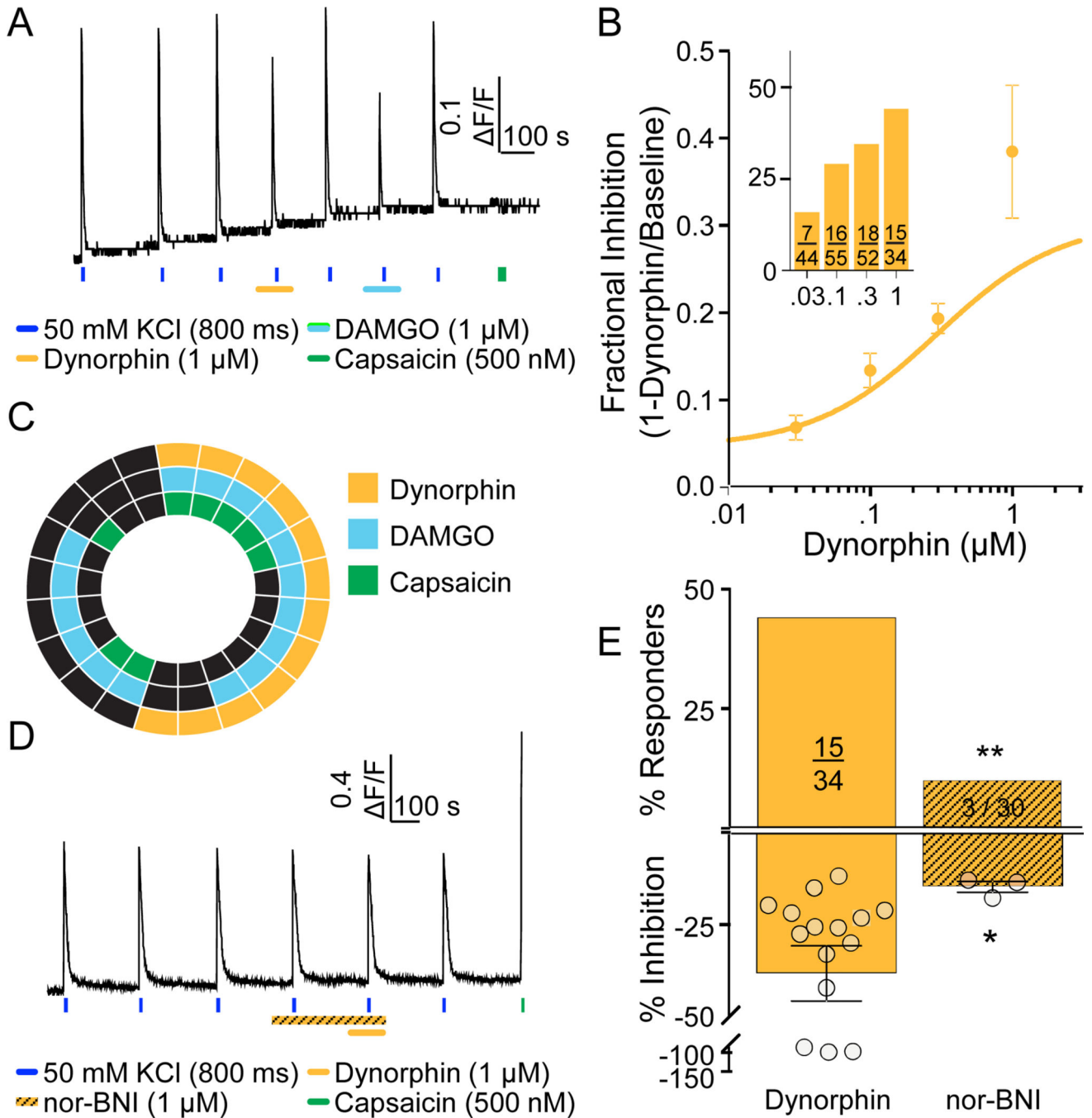


Figure 5. Characterization of functional KOP receptors in human DRG neurons.
A. Example of Ca^{2+} signaling in a neuron responsive to dynorphin and DAMGO, but not capsaicin. **B.** Both the magnitude of dynorphin-induced suppression of the evoked Ca^{2+} transient, and the proportion of neurons responsive to this KOP receptor agonist (inset), were concentration dependent. **C.** Distribution of neurons responsive to dynorphin, DAMGO, and capsaicin. **D.** Example of Ca^{2+} signaling in a neuron in which pre-application of the KOP receptor antagonist, nor-BNI was associated with the absence of a response to dynorphin. This neuron was responsive to capsaicin, however. **E.** Pooled data for neurons challenged

with dynorphin alone or following application of nor-BNI. The proportion of neurons responsive to dynorphin (** $p=0.0025$, chi-square) and the magnitude of the suppression of the evoked Ca^{2+} transient (* $p=0.027$, Mann Whitney t-test) were significantly reduced by nor-BNI.

Author Manuscript

Author Manuscript

Author Manuscript

Author Manuscript

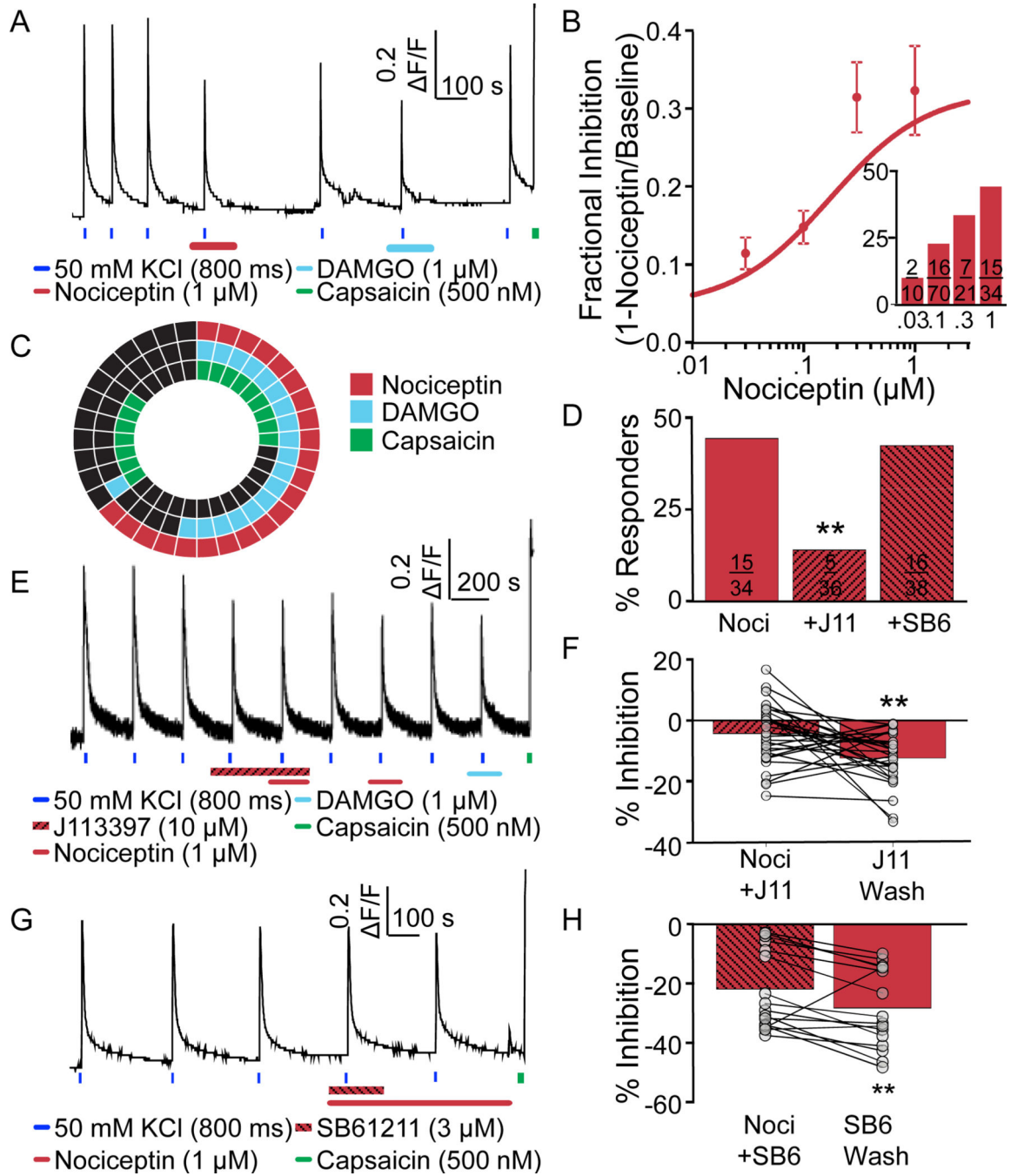


Figure 6. Characterization of functional NOP receptors in human DRG neurons.

A. Example of Ca^{2+} signaling in a neuron responsive to nociceptin. This neuron was also responsive to DAMGO and capsaicin. **B.** Pooled data indicate that both the magnitude of the nociceptin-induced suppression of the evoked Ca^{2+} transient and the proportion of neurons responsive to nociceptin (inset) was concentration dependent. **C.** The distribution of neurons responsive to nociceptin, DAMGO, and/or capsaicin. **D.** The proportion of neurons responsive to nociceptin when applied alone, or following application of the putative NOP receptor antagonists J113397 or SB612111 (J113397; ** $p=0.01$, chi-square). **E.** Example of

Ca²⁺ signaling in a neuron that was responsive to nociceptin following wash of J113397. **F.** Pooled magnitude of transient inhibition data from neurons treated with nociceptin in the presence of J113397, and again following wash of the antagonist ($t=2.977$, $df=28$, $**p=0.01$, paired t-test). **G.** Example of Ca²⁺ signaling in a neuron in which a nociceptin-induced decrease in the magnitude of the evoked transient was only detected following wash of the NOP receptor antagonist SB612111. **H.** Pooled data of neurons challenged with nociceptin in the presence of and then following wash of SB612111. The increase in the magnitude of the suppression of the evoked transient was significant (nociceptin [300nM] alone, $t=2.977$, $df=15$, $**p=0.01$, paired t-test).

Author Manuscript

Author Manuscript

Author Manuscript

Author Manuscript

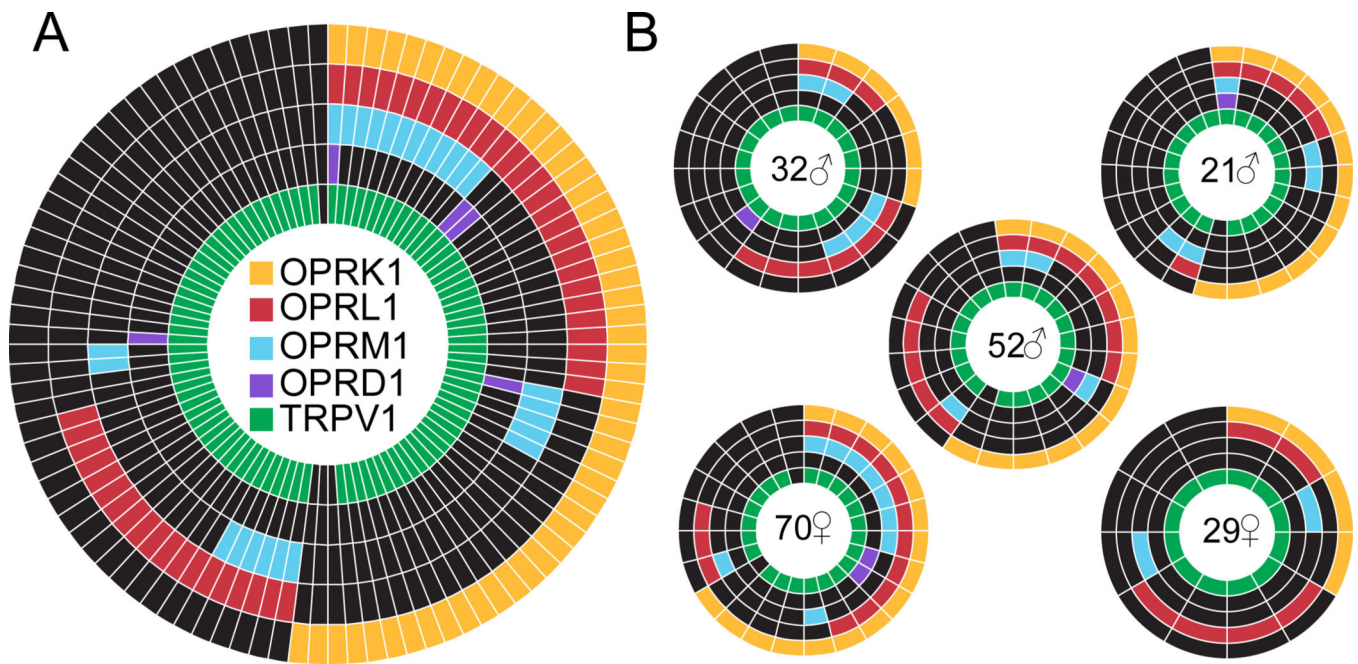


Figure 7. Expression of opioid receptor subtypes among human DRG neurons.

A. The pattern of opioid receptor subtype and TRPV1 expression in neurons pooled from five different organ donors. **B.** The sex and age of each donor is indicated in the center of each wheel. As with previous figures, each spoke is a single neuron, except that mRNA was assessed rather than functional responses to agonists. One donor was African American (29yo female).

Table 1.

Human donors

| Sex | Age (years) | BMI > 30 (% donors) | Hypertension (% donors) | Cigarette usage (% donors) | Previous drug usage (% donors) | Diabetic (% donors) |
|---------------|-----------------------------------------------------------------------------------|-------------------------|-------------------------|----------------------------|--------------------------------|---------------------|
| Female (n=23) | 47.3 ± 3.0 (2 African American, 21 Caucasian) | 39 (max = 50, min = 18) | 30 | 35 | 26 | 9 |
| Male (n=31) | 44.7 ± 3.0 (1 African American, 2 Asian American/ Pacific Islander, 28 Caucasian) | 39 (max = 38, min = 19) | 34 | 31 | 24 | 7 |

Age is mean ± SEM. BMI is body mass index. Hypertension includes both compliant and non-compliant with management protocol. Cigarette usage is any consistent usage even if donor stopped smoking. Previous drug use is any illegal drug use regardless of mode of intake. Diabetic includes any donor with the diagnosis of diabetes and includes types I and II and whether or not they were compliant with medical management.

Table 2.

Primer sequences used for single-cell semi-quantitative PCR.

| | |
|------------|---------------------------|
| GAPDH- Fwd | ACTCAGTCCCCACCACACT |
| GAPDH- Rev | GGTACATGACAAGGTGCGGC |
| LYS- Fwd | GCCATATCGGCTCGCAAATC |
| LYS- Rev | AACGAATGCCGAAACCTCCTC |
| OPRM1- Fwd | AGTGTGTTAGTTCCATCATCATGTC |
| OPRM1- Rev | TCTGATCATCCTGTCTACCTG |
| OPRD1- Fwd | CGGGACCTGTGGCTCTACAA |
| OPRD1- Rev | CCCCAACTCCGAAAGTCCG |
| OPRK1- Fwd | AATTCAGGGAGCACACTGGC |
| OPRK1- Rev | AAATGCGCTTAAGGAAGCTGGGT |
| OPRL1- Fwd | GGAAGTGATGGCTGTCTCGC |
| OPRL1- Rev | GAGCCTCCCAGAACAGTCC |
| TRPV1- Fwd | TTGGGGGTGTGGTGTTCCT |
| TRPV1- Rev | AGCAGGACTGGGGTTCCTAGA |

Forward (Fwd) and reverse (Rev) primers for glyceraldehyde 3-phosphate dehydrogenase (GAPDH), lysis protein (LYS), opioid receptor mu 1 (OPRM1), opioid receptor delta 1 (OPRD1), opioid receptor kappa (OPRK1), opioid related nociceptin receptor 1 (OPRL1), and transient receptor potential cation channel subfamily V member 1 (TRPV1).